



HAL
open science

Improving breast cancer sensitivity to paclitaxel by increasing aneuploidy

Sylvie Rodrigues-Ferreira, Anne Nehlig, Hadia Moindjie, Clarisse Monchecourt, Cynthia Seiler, Elisabetta Marangoni, Sophie Chateau-Joubert, Marie-Eglantine Dujaric, Nicolas Servant, Bernard Asselain, et al.

► **To cite this version:**

Sylvie Rodrigues-Ferreira, Anne Nehlig, Hadia Moindjie, Clarisse Monchecourt, Cynthia Seiler, et al.. Improving breast cancer sensitivity to paclitaxel by increasing aneuploidy. Proceedings of the National Academy of Sciences of the United States of America, 2019, 116 (47), pp.23691-23697. 10.1073/pnas.1910824116 . hal-02411561

HAL Id: hal-02411561

<https://univ-tlse2.hal.science/hal-02411561>

Submitted on 24 Nov 2020

HAL is a multi-disciplinary open access archive for the deposit and dissemination of scientific research documents, whether they are published or not. The documents may come from teaching and research institutions in France or abroad, or from public or private research centers.

L'archive ouverte pluridisciplinaire **HAL**, est destinée au dépôt et à la diffusion de documents scientifiques de niveau recherche, publiés ou non, émanant des établissements d'enseignement et de recherche français ou étrangers, des laboratoires publics ou privés.

Improving breast cancer sensitivity to paclitaxel by increasing aneuploidy

Sylvie Rodrigues-Ferreira^{1,2}, Anne Nehlig¹, Hadia Moindjie¹, Clarisse Monchecourt¹, Cynthia Seiler¹, Elisabetta Marangoni³, Sophie Chateau-Joubert⁴, Marie-Eglantine Dujaric⁵, Nicolas Servant⁶, Bernard Asselain⁵, Patricia de Cremoux⁷, Magali Lacroix-Triki⁸, Monica Arnedos⁸, Jean-Yves Pierga⁹, Fabrice André^{1,8}, and Clara Nahmias^{1*}

1. INSERM U981, LabEx LERMIT, Université Paris Sud, Gustave Roussy Research Center, Department of Molecular Medicine, 94800 Villejuif, France. 2. Present address : Inovarion SAS, 75013 Paris, France. 3. Laboratory of Preclinical Investigations, Translational Research Department, Institut Curie, PSL Research University, Paris, France. 4. BioPôle Alfort, Ecole Nationale Vétérinaire d'Alfort, Maisons Alfort, France. 5. Institut Curie, PSL Research University, Mines Paris Tech, Bioinformatics and Computational Systems Biology of Cancer, Paris, France. 6. Institut Curie, Unit of Biometry, PSL Research University, INSERM U900, Paris, France. 7. APHP Molecular Oncology Unit, Hôpital Saint Louis, Paris Diderot University, France. 8. Department of Medical Oncology, Gustave Roussy, 94800 Villejuif, France. 9. Medical Oncology Department, Institut Curie, Saint Cloud, Paris, France ; Université Paris Descartes, Sorbonne Paris Cite, Paris, France

Submitted to Proceedings of the National Academy of Sciences of the United States of America

Predictive biomarkers for tumor response to neoadjuvant chemotherapy are needed in breast cancer. This study investigates the predictive value of 280 genes encoding proteins that regulate microtubule assembly and function. By analyzing three independent multicenter randomized cohorts of breast cancer patients, we identified 17 genes that are differentially regulated in tumors achieving pathological complete response (pCR) to neoadjuvant chemotherapy. We focused on *MTUS1* gene, whose major product ATIP3 is a microtubule-associated protein down-regulated in aggressive breast tumors. We show here that low levels of ATIP3 are associated with increased pCR rate, pointing to ATIP3 as a new predictive biomarker of breast tumor chemosensitivity. Using preclinical models of patient-derived xenografts and 3D models of breast cancer cell lines, we show that low ATIP3 levels sensitize tumors to the effects of taxanes but not DNA-damaging agents. ATIP3 silencing improves the pro-apoptotic effects of paclitaxel and induces mitotic abnormalities, including centrosome amplification and multipolar spindle formation, which results in chromosome missegregation leading to aneuploidy. As shown by time-lapse videomicroscopy, ATIP3 depletion exacerbates cytokinesis failure and mitotic death induced by low doses of paclitaxel. Our results favor a mechanism by which the combination of ATIP3 deficiency and paclitaxel treatment induces excessive aneuploidy, which in turn results in elevated cell death. Together, these studies highlight ATIP3 as a new important regulator of mitotic integrity and a useful predictive biomarker for a population of chemoresistant breast cancer patients.

MTUS1 | predictive biomarker | taxanes | multipolar spindle | aneuploidy

Introduction

Breast cancer is a leading cause of cancer death among women worldwide. Neo-adjuvant chemotherapy, administered before surgery, represents an option for a number of breast cancer patients (1). Pre-operative chemotherapy decreases primary tumor burden, thus facilitating breast conservation (2, 3), and administration of chemotherapy on naïve tumors prior to surgery also provides the opportunity to rapidly measure tumor response and identify breast cancer patients that may gain advantage from the treatment. The achievement of pathological complete response (pCR), characterized by complete eradication of all invasive cancer cells from the breast and axillary lymph nodes, is often considered as a surrogate endpoint for cancer-free survival after neoadjuvant setting, especially in aggressive triple-negative breast tumors (4,5). Clinical parameters, such as estrogen receptor-negative status, high histological grade and high proliferative status have been associated with greater sensitivity to chemotherapy (5,6). However, the proportion of patients who achieve a pCR fol-

lowing preoperative chemotherapy remains low, reaching 15-20% in the whole population and 30-40% in ER-negative tumors (7,8). Considering the rapidly growing area of personalized medicine, the identification of efficient molecular markers that can predict sensitivity to chemotherapy is crucial to select the patients who may benefit from therapy, thereby avoiding unnecessary treatment and associated toxicities for those who remain resistant (9).

The most used regimens in the neoadjuvant setting of breast cancer patients include taxanes and anthracyclines, which combination is associated with improved outcome compared to anthracyclines alone (3). Taxanes (paclitaxel and docetaxel) are microtubule-targeting agents that bind and stabilize microtubules (MT), inducing mitotic arrest and apoptosis (10, 11). At clinically relevant concentrations of the nanomolar range, these drugs suppress MT dynamic instability (11-13) and behave as mitotic poisons that target the mitotic spindle during mitosis, inducing multipolar spindles and centrosomal abnormalities (13). The assembly and dynamics of the mitotic spindle are tightly regulated by a number of MT-associated proteins (MAP) and mitotic kinases (14, 15), suggesting that alterations of MAP expression and/or function in breast tumors may regulate their sensitivity to taxane-based chemotherapy. Gene expression studies indeed identified the MAP tau protein as a predictive biomarker whose down-regulation is associated with increased pCR rate in breast cancer patients (16-21), underlining the interest of studying MT-regulating proteins as new predictors of chemotherapy efficacy.

Significance

Low levels of ATIP3 in breast tumors are associated with increased response to neoadjuvant chemotherapy and ATIP3 silencing in breast cancer cells potentiates the effects of paclitaxel, highlighting the importance of this predictive biomarker to select breast cancer patients who are sensitive to taxane-based chemotherapy. ATIP3 depletion promotes mitotic abnormalities including centrosome amplification and multipolar spindle formation, which is a source of chromosome segregation errors and aneuploidy. Excessive aneuploidy in ATIP3-deficient cells treated with low doses of paclitaxel results in massive cell death.

Reserved for Publication Footnotes

137
138
139
140
141
142
143
144
145
146
147
148
149
150
151
152
153
154
155
156
157
158
159
160
161
162
163
164
165
166
167
168
169
170
171
172
173
174
175
176
177
178
179
180
181
182
183
184
185
186
187
188
189
190
191
192
193
194
195
196
197
198
199
200
201
202
203
204

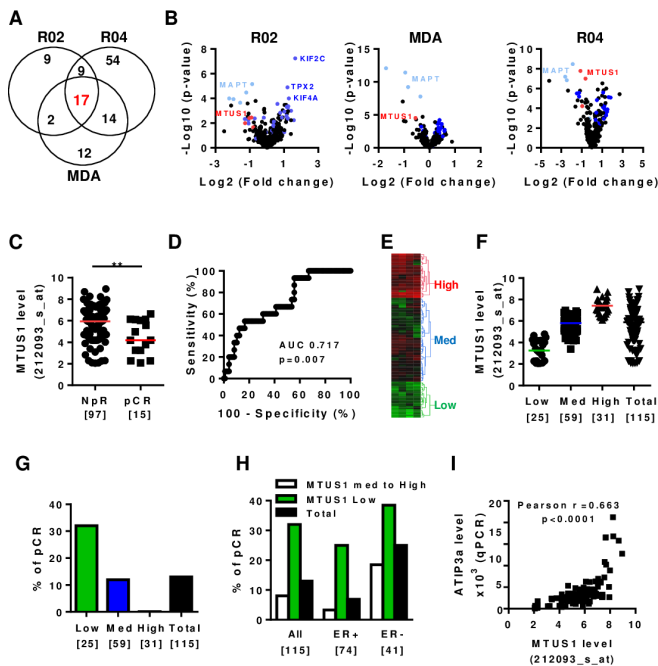


Figure 1

Fig. 1. A-Venn diagram of the number of differentially expressed genes between sensitive (pathological complete response, pCR) and resistant tumors (Non pathological response, NpR) in each of the three cohorts; REMAGUS02 (R02), REMAGUS04 (R04) and M.D. Anderson (MDA), and common genes among them. B- Volcano plots showing differentially expressed genes between sensitive (pCR) and resistant tumors (NpR) from patients of the R02 (left), MDA (middle) and R04 (right) cohorts. Each dot represents the fold change and the p-value obtained for a single gene probeset. Genes common to all three cohorts are plotted in blue. *MAPT* is plotted in light blue and *MTUS1* is in red. Names of the best candidates are indicated. C- Scattered dot plot of *MTUS1* probeset (212093.s.at) intensity in tumors from patients of the R02 cohort with no pathological response (NpR) or achieving pathological complete response (pCR) after neoadjuvant chemotherapy. Numbers of samples are indicated under brackets. ** $p < 0.01$. D- ROC curve evaluating the performance of *MTUS1* expression for predicting complete response to neoadjuvant chemotherapy. AUC Area Under the Curve. E- Heat-map and hierarchical clustering of 115 breast tumor samples based on the intensities of four *MTUS1* probesets (212096.s.at; 212093.s.at; 212095.s.at 239576.at). Heat-map illustrates relative expression profiles of *MTUS1* (column) for each tumor sample (line) in continuous color scale from low (green) to high (red) expression. Dendrogram of the 3 selected tumor groups is shown on the right. F- Scattered dot plot of *MTUS1* expression in each of the 3 selected clusters based on the dendrogram shown in (E). Numbers of samples are under brackets. G- Proportion of patients with pCR according to *MTUS1* level in each selected cluster. Numbers of tumors in each group are indicated under brackets. H- Proportion of patients with pCR according to *MTUS1* level in all tumors (All) and among ER+ and ER- tumors. Numbers of tumors in each group are indicated under brackets. I- Correlation between *MTUS1* (212093.s.at) probeset intensities and *ATIP3* mRNA levels measured by real-time RT-PCR (qPCR) using oligonucleotides designed in 5' exons that are specific to *ATIP3* transcripts, in 106 breast tumor samples of the R02 cohort.

In the present study, we analyzed a panel of 280 genes encoding MT-regulating proteins to evaluate their predictive value as biomarkers of neoadjuvant taxane-based chemotherapy in breast cancer patients. Seventeen genes were identified as being

205
206
207
208
209
210
211
212
213
214
215
216
217
218
219
220
221
222
223
224
225
226
227
228
229
230
231
232
233
234
235
236
237
238
239
240
241
242
243
244
245
246
247
248
249
250
251
252
253
254
255
256
257
258
259
260
261
262
263
264
265
266
267
268
269
270
271
272

Table 1. MT-regulating genes differentially expressed in chemosensitive breast tumors

Gene Symbol	Gene Name	Process
<i>ASPM</i>	Abnormal spindle microtubule assembly	MT minus-end binding, spindle organization
<i>AURKB</i>	Aurora kinase B	Ser/Thr protein kinase, spindle organization
<i>GTSE1</i>	G2 and S phase-expressed 1	MT plus-end binding, spindle organization, cell migration
<i>KIF11</i>	Kinesin family member 11	MT molecular motor activity, spindle organization
<i>KIF14</i>	Kinesin family member 14	MT molecular motor activity
<i>KIF15</i>	Kinesin family member 15	MT molecular motor activity
<i>KIF18B</i>	Kinesin family member 18B	MT depolymerizing activity, spindle organization
<i>KIF20A</i>	Kinesin family member 20A	MT molecular motor activity
<i>KIF2C</i>	Kinesin family member 2C	MT depolymerizing activity, spindle organization
<i>KIF4A</i>	Kinesin family member 4A	MT molecular motor activity, chromokinesis
<i>KIFC1</i>	Kinesin family member C1	MT molecular motor activity, spindle assembly
<i>RACGAP1</i>	Rac GTPase-activating protein 1	MT plus-end binding, spindle midzone assembly, cytokinesis
<i>STMN1</i>	Stathmin 1	MT-destabilizing protein, spindle organization
<i>TPX2</i>	Targeting protein for Xklp2	Aurora kinase A-regulator, spindle organization
<i>MAPT</i>	Microtubule-associated protein tau	MT-stabilizing protein, EB1-binding
<i>MAST4</i>	Microtubule associated serine/threonine kinase family member 4	Ser/Thr protein kinase
<i>MTUS1</i>	Microtubule-associated tumor suppressor 1	MT-stabilizing protein, EB1-binding, tumor-suppressor effects

Properties of the 17 differentially regulated MT-regulating genes common to the REMAGUS02 (R02, left), M.D. Anderson (MDA, middle), and REMAGUS04 (R04, right) studies. Genes up-regulated in sensitive (pCR) tumors are in yellow, those down regulated are in blue.

Table 2. Predictive factors of pathological complete response (pCR) in the R02 study

Variable	Univariate		Multivariate		
	pCR (%)	OR (95%CI)	pvalue	OR (95%CI)	pvalue
Age					
<50	8 (10.3)	0.44 (0.145-1.33)	0.147		
>50	7 (20.6)				
ER					
negative	10 (25)	4.46 (1.4-14.2)	0.011	4.66 (1.46-14.81)	0.0076
positive	5 (6.9)				
PR					
negative	13 (21.3)	6.5 (1.39-30.36)	0.017	1.88 (0.40-8.78)	0.281
positive	2 (4)				
HER2					
negative	9 (12.2)	1.35 (0.11-4.13)	0.597		
positive	6 (15.8)				
Grade					
III	10 (16.1)	2.01 (0.59-6.89)	0.262		
I/II	4 (8.7)				
Tumor stage					
T2	10 (17.8)	2.21 (0.70-6.96)	0.172		
T3-4	5 (8.9)				
Nodal Status					
N0	8 (19.1)	2.05 (0.684-6.14)	0.199		
N+	7 (10.3)				
MTUS1 level					
low	8 (32)	5.37 (1.71-16.84)	0.0039	12.16 (3.88-38.07)	<0.0001
med (n=7) high	7 (8.1)				
(n=0)					
continuous *		1,78 (1.19-2.76)	0,005		

* Entered as continuous variable (probeset 212096_s.at values)
Univariate and multivariate analysis are shown on the left and right, respectively.

differentially expressed in tumors from patients achieving pCR from three independent multicenter randomized breast cancer clinical trials. We focused our interest on candidate tumor suppressor gene *MTUS1* (22, 23) that encodes the MT-stabilizing protein ATIP3, previously reported as a prognostic biomarker of breast cancer patient survival (24, 25). We show here that low ATIP3 expression in breast tumors is associated with higher pCR rate. Unexpectedly, ATIP3 deficiency, which is known to increase MT instability (25), improves rather than impairs cancer cell sensitivity to taxanes. Our results favor a model in which ATIP3 depletion sensitizes cancer cells to paclitaxel by increasing centrosome amplification and mitotic abnormalities, leading to massive aneuploidy and cell death.

Results

Gene expression studies identify *MTUS1* gene as a predictor of breast tumor response to neoadjuvant chemotherapy

To identify new predictive biomarkers of sensitivity to neoadjuvant chemotherapy in breast cancer, we analyzed a panel of 280 genes encoding MT-regulatory proteins including MAPs and mitotic kinases. We compared gene expression profiles with clinical data in three independent cohorts (R02, MDA and R04) of 115, 133 and 142 breast cancer patients, respectively (dataset Table S1). We identified a total of 118 genes that were significantly differentially regulated ($p < 0.01$) in patients who achieved pCR compared to those (NpR) who did not. Among them, 17 were common to all three cohorts (Fig.1A, 1B, Table 1, dataset Table S2). These genes encode structural MAPs that regulate MT stability (*MAPT*, *MTUS1*, *STMN1*), MT end-binding proteins (*ASPM*, *GTSE1*, *RACGAP1*), protein kinases and their regulators (*AURKB*, *MAST4*, *TPX2*) and molecular motors (a total of 8 kinesins) that control mitosis, cytokinesis or intracellular trans-

port. Of note, the MT-stabilizing protein tau encoded by *MAPT* was previously described as a potent predictor of taxane-based chemotherapy in breast cancer (16-21), therefore validating our gene profiling approach.

Besides *MAPT*, the *MTUS1* gene consistently reached higher fold change and better p value in all three cohorts (Fig. 1B). We thus focused our attention on *MTUS1*, whose gene product ATIP3 has been identified as a prognostic biomarker of patient survival with potent tumor suppressor effects in breast cancer (24, 25). In each cohort of breast cancer patients examined, *MTUS1* Affymetrix probesets intensities were significantly lower in cases with pCR than in those with NpR (Fig.1C, datasets Fig S1-S3). Receiver Operating Curves (ROC) revealed an Area under the curve (AUC) values of 0.717 ($p=0.007$), 0.699 ($p=0.0005$) and 0.769 ($p<0.0001$) in the R02, MDA and R04 cohorts, respectively, indicating that *MTUS1* levels predict the response to chemotherapy with good accuracy (Fig 1D, datasets Fig S1-S3).

Tumors were then classified into three groups expressing high, medium and low *MTUS1* levels according to heatmap hierarchical clustering (Fig 1E, 1F). In the R02 cohort, the pCR rate was 32% (8/25) in tumors expressing low *MTUS1* levels compared to 11.9% (7/59) and 0% (0/31) in those expressing medium and high levels of *MTUS1*, respectively (Fig 1G), indicating that the subpopulation of low *MTUS1*-expressing tumors is more prone to achieve complete response. Of note, 100% of tumors with high *MTUS1* levels failed to achieve pCR, suggesting that high *MTUS1* levels may identify patients unlikely to respond to chemotherapeutic treatment (Fig 1G). Similar results were obtained using the two other cohorts of patients (datasets Fig S2D, S3D).

Univariate logistic regression analysis including age, hormone receptors, HER2, tumor grade, stage, nodal status and *MTUS1* level identified hormonal receptors ER (OR 4.46; CI[1.4-14.2])

409
410
411
412
413
414
415
416
417
418
419
420
421
422
423
424
425
426
427
428
429
430
431
432
433
434
435
436
437
438
439
440
441
442
443
444
445
446
447
448
449
450
451
452
453
454
455
456
457
458
459
460
461
462
463
464
465
466
467
468
469
470
471
472
473
474
475
476

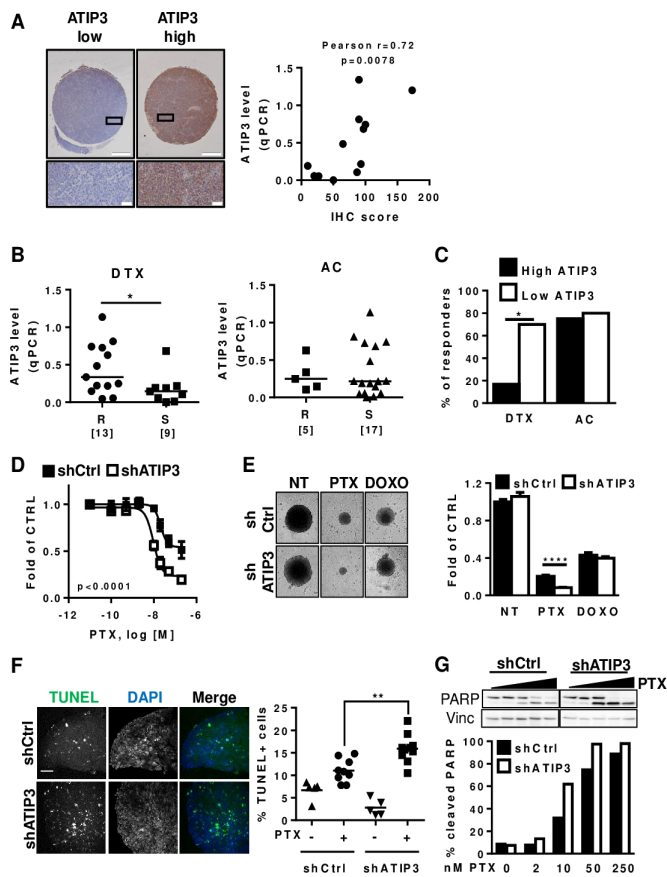


Figure 2

Fig. 2. A- Left: Immunohistochemistry performed on human breast cancer xenograft sections of a Tissue Microarray (TMA) using anti-MTUS1 monoclonal antibody. Shown are representative photographs of tumors expressing low (left) or high (right) levels of ATIP3. A bar represents 500µm. Insets are shown in the bottom with a bar representing 50µm. **Right:** Correlation between ATIP3 mRNA expression level (by qPCR) and Immunohistochemistry score (IHC score). **B-** Scattered dot plot of ATIP3 (qPCR) mRNA expression level in HBCx treated with Docetaxel (DTX) (left panel) or with Anthracycline-Cyclophosphamide (AC) (right panel). Tumors are classified according to their response to drug treatment. R indicates resistance and S indicates sensitivity to the treatment. Numbers of samples are under brackets. * $p < 0.05$ **C-** Percentage of responsive HBCx according to ATIP3 level. Tumors were subdivided into groups expressing high-ATIP3 versus low-ATIP3 levels based on the median value of ATIP3 measured by real-time RT-PCR. * $p < 0.05$ **D-** Dose response curves of SUM52PE spheroids expressing (shCtrl) or not (shATIP3) ATIP3 and treated with increasing concentrations of Paclitaxel (PTX). **E-** SUM52PE spheroids expressing (shCtrl) or not (shATIP3) ATIP3 were treated for 6 days with 50nM Paclitaxel (PTX) or 100nM Doxorubicin (DOXO) and photographed. Picture represents one spheroid of the quadruplicate. Spheroid area were measured and results are plotted in the histogram on the right. **** $p < 0.0001$ **F-** Representative photographs of SUM52PE spheroids expressing endogenous ATIP3 (shCtrl) or silenced by shRNA (shATIP3) treated with 50nM of PTX for 72hrs prior to staining with TUNEL reagent (green) and DAPI (blue). Quantification of apoptosis, measured as percent of TUNEL-positive cells, is shown on the right. Obj x20, scale bar 100µm. ** $p < 0.01$ **G-** Western Blot analysis of PARP cleavage in SUM52PE spheroid expressing (shCtrl) or not (shATIP3) ATIP3 treated for 72hrs with increasing concentrations of PTX. Vinculin (Vinc) is used as internal loading control. Quantification is shown below.

and PR (OR 6.5; CI[1.39-30.36]), as well as *MTUS1* (OR 5.37; CI[1.71-16.84]) as predictive factors associated with pCR after neoadjuvant chemotherapy (Table 2, dataset Table S3). In multivariate analysis, ER (OR 4.66; CI[1.46-14.81]) and *MTUS1* (OR

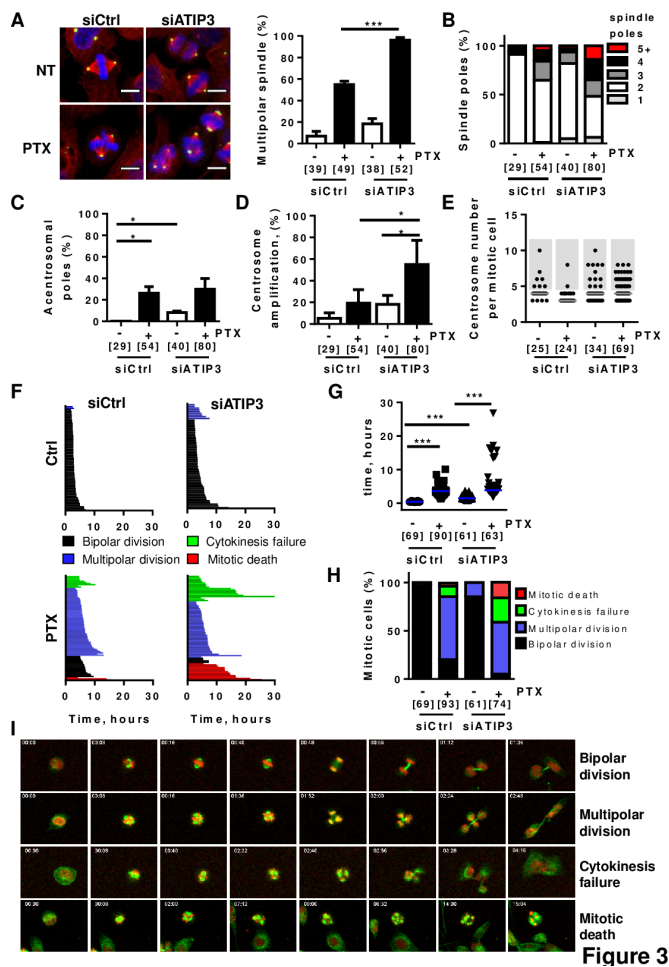


Figure 3

Fig. 3. A. Immunofluorescence photographs of HeLa cells transfected with siCtrl or siATIP3 and treated or not with 5nM of PTX prior to staining with antibodies directed against α -tubulin (red) and pericentrin (green). Nuclei are stained with DAPI (blue). Quantification of abnormal mitoses is shown on the right. **B.** Proportion of mitotic HeLa cells with abnormal number of spindle poles upon 48 hrs ATIP3 silencing and 18hrs PTX treatment (2nM). **C.** Percent of mitotic HeLa cells containing acentrosomal poles. Cells were treated as in B. **D.** Percent of mitotic HeLa cells containing more than two centrosomes. Cells were treated as in B. **E.** Scattered dot plot of the number of centrosomes per mitotic HeLa cells treated as in B. **F.** Cell fate profiles of control (left) and ATIP3-silenced (right) HeLa cells in absence (top) or in presence of 2nM PTX (bottom). **G.** Scattered dot plot of mitotic length measured from chromosome condensation to initiation of cytokinesis in HeLa cells silenced or not for ATIP3 and treated or not with 2nM PTX. **H.** Proportion of cell fate profiles measured in F. **I.** Images from time lapse experiment performed in F, showing representative cell fates. Microtubules are stained in green, DNA in red. Time, hours:minutes, is indicated in upper left of the picture. **A-H.** Number of mitotic cells is under brackets. * $p < 0.05$, *** $p < 0.001$

12.16; CI[3.88-38.07]) were identified as independent predictors of pCR (Table 2, dataset Table S3). These results indicate that low *MTUS1* status may be used to identify patients with high response rates. Notably, 32% of low-*MTUS1* tumors were associated with pCR, compared to 25% for ER-negative tumors. Combining ER status and low *MTUS1* levels further increased the pCR rate from 7% to 25% among ER-positive tumors, and 25% to 39% among ER-negative tumors of the R02 cohort (Fig 1H). Similar results were obtained with the two other series of patients (datasets Fig. S2E, S3E). Real time RT-PCR analysis performed in a panel of 106 breast tumors of the R02 cohort using 3 different pairs of oligonucleotides showed significant correlation between ATIP3 mRNA levels and *MTUS1* Affymetrix probe intensities

477
478
479
480
481
482
483
484
485
486
487
488
489
490
491
492
493
494
495
496
497
498
499
500
501
502
503
504
505
506
507
508
509
510
511
512
513
514
515
516
517
518
519
520
521
522
523
524
525
526
527
528
529
530
531
532
533
534
535
536
537
538
539
540
541
542
543
544

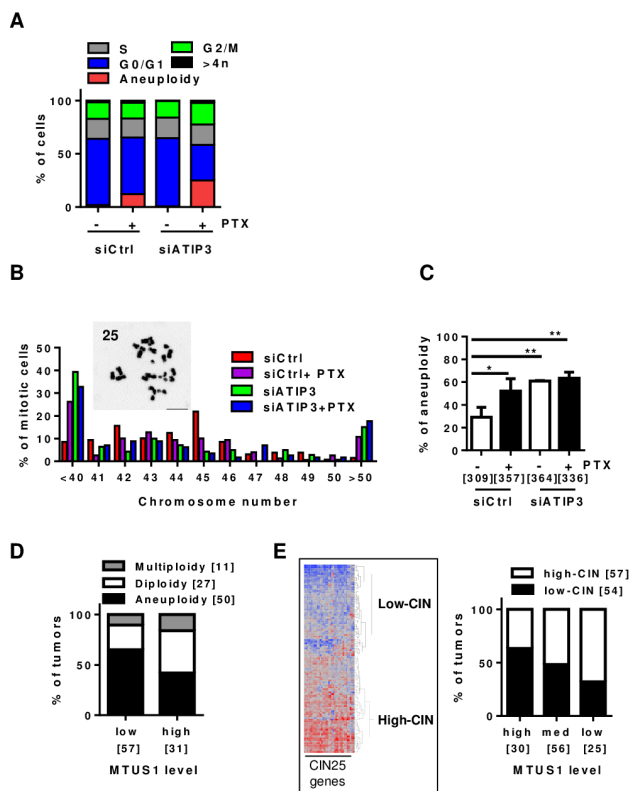


Figure 4

Fig. 4. A. FACS analysis of DNA content of HeLa cells transfected with scramble or ATIP3-directed siRNA prior treatment with 5nM PTX for 18h. Shown is the proportion of cells in each cell cycle fraction. B. Proportion of HCT116 metaphase spreads containing abnormal numbers of chromosomes. Inset shows a representative image of metaphase spread and corresponding number of chromosomes is indicated in the upper left corner of the image. C. Percentage of aneuploid cells among HCT116 cells silenced (siATIP3) or not (siCtrl) for ATIP3 and treated or not with 5nM PTX for 18hrs. Number of metaphase spreads analyzed in 3 independent experiments is shown under brackets. * $p < 0.05$, ** $p < 0.01$. D. Proportion of tumors from the Curie cohort showing altered ploidy according to ATIP3 level. Number of tumors analyzed is indicated under brackets. E. Heatmap and hierarchical clustering of 115 breast tumor samples of the R02 study based on the intensities of the 25 genes from chromosomal Instability CIN signature (29). Proportion of tumors expressing high level (high-CIN) or low levels (low-CIN) of CIN signature according to ATIP3 levels is shown on the right. Number of tumors is indicated under brackets

(Fig 1I, datasets Fig S1D-S1F). Together, these results indicate that low ATIP3 mRNA levels predict breast tumor response to chemotherapy.

Low ATIP3 expression in breast tumors and cancer cells increases sensitivity to taxanes but not DNA-targeting agents

Pre-clinical studies were undertaken using patient-derived xenografts (26) to confirm and extend our results obtained on breast cancer patients. Twenty-two models of human breast cancer xenografts grown in mice (HBCx) were exposed to either Docetaxel (DTX) or Anthracycline plus Cyclophosphamide (AC). ATIP3 expression levels in HBCx were evaluated by real time RT-PCR and validated by IHC (Fig 2A, dataset Table S4). ATIP3 mRNA levels were then plotted according to sensitivity (S) or resistance (R) of tumors to DTX and AC treatment. As shown

in Fig 2B, DTX-sensitive xenografts displayed significantly lower ATIP3 levels than DTX-resistant ones (median expression value 0.14 versus 0.33). No significant difference in ATIP3 level was observed between AC-sensitive and AC-resistant HBCx (Fig 2B), indicating that ATIP3 levels are associated with the response to the microtubule-targeting agent DTX rather than to DNA-targeting drugs. Accordingly, the response rate to DTX was significantly higher in low-ATIP3 compared to high-ATIP3 expressing HBXs (70% vs 16.7%) whereas the response rate to AC remained similar in both groups of tumors (80% vs 75%) (Fig 2C).

We then investigated the consequence of ATIP3 depletion on breast cancer cell viability upon exposure to chemotherapy. Breast cancer cells were grown in 3-dimensions as multicellular spheroids to mimic the main features and tissue architecture of solid tumors (27) and were treated with increasing doses of chemotherapeutic agents. ATIP3 silencing in SUM52-PE cells (dataset Fig S4A) markedly improved the cytotoxic effects of both docetaxel (DTX) and paclitaxel (PTX) (Fig 2D, datasets Fig S4B-S4D) but had no effect on the cellular response to doxorubicin (Fig 2E). Similar results were obtained in HCC1143 and MDA-MB-231 breast cancer cells treated with DTX and PTX, respectively (datasets Fig S4E, S4F), confirming that ATIP3-deficiency sensitizes breast cancer cells to taxanes but not to DNA-targeting drugs.

Taxanes are mitotic poisons that arrest cells in mitosis and trigger apoptosis. Multicellular spheroids treated with clinically relevant doses of PTX (13) were arrested in mitosis, a phenotype that was further increased in ATIP3-deficient cells (dataset Fig.S5A). ATIP3-deficiency also increased the percentage of cells undergoing apoptosis following treatment with low doses of PTX (Fig 2F, dataset Fig S5B). Accordingly, molecular markers of apoptosis, such as cleavage of PARP (Fig 2G) and of caspase-3 (dataset Fig S5C) as well as decline in anti-apoptotic protein Mcl-1 levels (dataset Fig S5D), were elevated upon PTX treatment in ATIP3-deficient compared to ATIP3-proficient spheroids. Thus, ATIP3 deficiency improves the mitotic and pro-apoptotic effects of taxanes.

PTX-induced mitotic defects are increased in ATIP3-deficient cells

To get insight into the mechanism by which ATIP3 depletion sensitizes cancer cells to the effects of PTX, we examined the consequences of ATIP3 silencing on mitosis. HeLa cells were used as a reference model in these experiments because they express endogenous ATIP3 and are more suitable than SUM52 cells for cell imaging. As shown in Fig.3A, ATIP3 depletion induced the formation of multipolar spindles (18%) and raised from 55% to almost 100% the percentage of multipolar cells in the presence of low doses of PTX. ATIP3 depletion also markedly increased the number of spindle poles formed upon PTX treatment, with a significant fraction of spindles showing more than 5 poles (Fig 3B), some of them being acentrosomal (Fig 3C), indicating excessive mitotic abnormalities. The increased number of spindle poles was mainly due to centrosome amplification which was markedly increased when combining ATIP3-silencing and PTX treatment (Fig 3D). Accordingly, ATIP3 silencing was associated with supernumerary centrosomes and the number of centrosomes per mitotic cell was further elevated in ATIP3-deficient cells upon PTX treatment (Fig 3E, dataset Fig S6A). More than half of supernumerary centrosomes contained either one or no centriole (dataset Fig S6B), underlining major centrosomal defects. Together these results indicate that ATIP3 silencing induces centrosome amplification leading to multipolar spindles, a phenotype that is amplified upon PTX treatment.

We then examined the consequences of ATIP3 silencing and PTX treatment on cell fate at the single cell level using time-lapse videomicroscopy (Fig 3F, datasets movies 1-4). ATIP3-silencing increased the time in mitosis (Fig 3G) and induced the formation

681 of multipolar cells that were able to divide, giving rise to 2 or 3
682 viable daughter cells containing several nuclei (Fig 3H, 3I, dataset
683 movie 2). PTX at low dose induced a majority (79%) of cells with
684 multipolar spindles, among which 14% were unable to divide.
685 These cells either died in mitosis or underwent cytokinesis failure,
686 giving rise to groups of multinucleated cells that ultimately died
687 during the following division (Fig 3H, 3I, dataset movie 3). ATIP3-
688 silencing combined with low dose of PTX induced massive (95%)
689 formation of multipolar cells, 41% of which died during the first
690 division from cytokinesis failure or mitotic death (Fig 3H, 3I,
691 dataset movie 4). Thus, ATIP3 silencing exacerbates mitotic ab-
692 normalities and subsequent cell death induced by PTX treatment.

ATIP3 depletion is associated with increased aneuploidy

693 The formation of multipolar spindles is a source of chromo-
694 some missegregation and aneuploidy, suggesting that ATIP3
695 silencing may promote aneuploidy. To test this hypothesis, we
696 analyzed cellular DNA content by flow cytometry to assess DNA
697 ploidy in HeLa cells treated or not with low doses of PTX. In
698 line with previous studies (11, 13), treatment with PTX at the
699 nanomolar range resulted in a hypodiploid (<2N) population of
700 cells (Fig 4A, dataset Fig S7A). This population of aneuploid cells
701 disappeared at higher concentrations of PTX (100 nM) when cells
702 were arrested in G2/M (dataset Fig S7B) and was negative for
703 Annexin-V labelling (dataset Fig S7C), excluding the possibility
704 that these cells may be apoptotic. In ATIP3 depleted cells, hy-
705 podiploidy could not be detected by flow cytometry procedures
706 in the absence of treatment (Fig 4A). However, following PTX
707 exposure, the population of hypodiploid cells was raised from 12
708 % in control cells to 25% in ATIP3-deficient cells, indicating that
709 ATIP3-silencing increases PTX-induced aneuploidy.

710 Aneuploidy was also evaluated by counting chromosome
711 number per cell, in metaphase chromosome spreads of HCT116
712 cells, used as a reference cellular model in these studies because
713 they are nearly diploid and chromosomally stable. PTX treatment
714 significantly increased the incidence of both hypodiploid (<40
715 chromosomes) and hyperdiploid (>50 chromosomes) cells and
716 ATIP3 silencing further increased aneuploidy (Fig 4B, 4C).

717 To assess the clinical relevance of our findings, we analyzed
718 a series of 88 breast cancer patients in which ploidy had been
719 evaluated. Tumors were grouped according to low- and high-
720 *MTUS1* level using heatmap classification as reported (24, 28)
721 and compared with ploidy status (dataset Table S5). As shown
722 in Fig 4D, 65% of low-*MTUS1* tumors were found to be aneu-
723 ploidy compared to 42% of high-*MTUS1* tumors. Since aneu-
724 ploidy often results from chromosomal instability (CIN), we
725 investigated whether *MTUS1* levels may also be associated with
726 CIN. A "CIN25 signature", comprising a panel of 25 differentially
727 regulated genes has previously been reported in breast cancer
728 (29). We therefore classified breast tumors as high-CIN or low-
729 CIN based on the "CIN25 signature" and compared the signature
730 with *MTUS1* levels. As shown in Fig 4E and dataset Fig S8,
731 40% of breast tumors with high-*MTUS1* levels were classified
732 as high-CIN compared to 60% of low-*MTUS1* tumors. Together,
733 these results comfort the notion that breast tumors expressing low
734 levels of ATIP3 are more prone to chromosomal instability and
735 aneuploidy.

Discussion

736 Based on transcriptional profiling of three independent cohorts
737 of breast cancer patients treated with taxane-based neoadjuvant
738 chemotherapy, we show here for the first time that microtubule-
739 associated protein ATIP3 is an independent predictive biomarker
740 of the response to treatment. Low levels of ATIP3 were signifi-
741 cantly more frequent in breast tumors that achieved pCR com-
742 pared with those that did not respond to treatment, suggesting
743 that low ATIP3 expression may be used as a marker to iden-
744 tify breast cancers that are highly sensitive to taxane-containing

745 chemotherapy. Importantly, in all three cohorts analyzed, 98% to
746 100% of tumors expressing high levels of ATIP3 failed to achieve
747 pCR, indicating that ATIP3 may also be a useful biomarker to
748 select patients unlikely to respond to conventional chemotherapy,
749 which is of clinical importance to limit toxicity and side effects of
750 ineffective treatments. Low ATIP3 levels predict the response to
751 neoadjuvant chemotherapy even better than ER-negative status
752 and can further identify responders among ER-negative tumors.
753 This finding is of particular interest for triple-negative breast
754 tumors (TNBC) for which chemotherapy remains the unique
755 therapeutic option (30). Further validation in adjuvant trials is
756 warranted to firmly establish the value of ATIP3 as a predictive
757 biomarker in clinical practice in breast cancer. It will be inter-
758 esting to broaden our study to other types of malignancies, such
759 as prostate, lung or ovarian cancer, where taxanes are frequently
760 used.

761 Pre-clinical studies performed on breast cancer patients-
762 derived xenografts and in 3D-models of multicellular spheroids
763 further allowed us to investigate the predictive value of ATIP3 in
764 the response to taxanes compared to anthracyclines and showed
765 that low levels of ATIP3 are associated with high sensitivity to
766 docetaxel, with no impact on the response to DNA-targeting
767 agents. Accordingly, ATIP3-silencing sensitizes cancer cells to low
768 doses of paclitaxel and potentiates the well-known effects of the
769 drug on mitotic arrest and apoptosis. Although consistent with
770 data from breast cancer patients, this was an unexpected result
771 given that ATIP3 silencing increases MT dynamics (25), which is
772 opposite to the MT-stabilizing effects of taxanes.

773 Results presented here indicate that silencing of the MT-
774 stabilizing protein ATIP3 induces multiple mitotic abnormalities
775 that mimic those induced by PTX. We propose a mechanism in
776 which ATIP3 silencing, by causing centrosome amplification and
777 multipolar spindle formation, amplifies the effects of taxanes and
778 thereby exacerbates mitotic abnormalities, chromosome segrega-
779 tion errors, CIN features and aneuploidy, ultimately leading to
780 cell death in response to treatment.

781 It has been widely shown that centrosome amplification,
782 leading to spindle multipolarity and subsequent chromosome
783 missegregation and aneuploidy, promotes tumor initiation and
784 progression (31-33). Centrosome amplification is also associated
785 with worse clinical outcome in breast cancer (34, 35). In this
786 context, our findings that ATIP3 deficiency induces centrosome
787 amplification are consistent with previous observations that low
788 ATIP3 levels in breast tumors are associated with poor patient
789 prognosis (25). Strikingly, our data also indicate that combining
790 ATIP3 deficiency and PTX treatment causes excessive centro-
791 some amplification and aneuploidy, which in turn triggers massive
792 cell death in mitosis. This is in line with previous observations that
793 increasing chromosome missegregation and aneuploidy beyond a
794 critical threshold leads to cancer cell death and tumor suppression
795 (36, 37), and supports our clinical results showing higher pCR for
796 ATIP3-deficient breast cancer patients treated with taxane-based
797 chemotherapy.

798 In conclusion, while the consequences of centrosome ampli-
799 fication and CIN for therapeutic responses in cancer patients still
800 remain a matter of debate (38), our data emphasize for the first
801 time the link between centrosome amplification and increased
802 pCR rates for breast tumors. Our results highlight ATIP3 as a
803 novel predictive biomarker to select a population of breast cancer
804 patients who are likely to benefit from taxane-based chemother-
805 apy and open the way to new therapeutic strategies based on
806 increasing centrosomal alterations to achieve chemosensitivity.

Materials and Methods

807 Studies using cohorts of patients and patient-derived xenografts were re-
808 viewed by ethical committees and approved by institutional review boards.
809 All patients signed an informed consent for voluntary participation in the
810 trial. Details on patients and samples, clinical data and gene profiling are
811 provided in Supporting Materials and Methods. These also describe RNA
812

817
818
819
820
821
822
823
824
825
826
827
828
829
830
831
832
833
834
835
836
837
838
839
840
841
842
843
844
845
846
847
848
849
850
851
852
853
854
855
856
857
858
859
860
861
862
863
864
865
866
867
868
869
870
871
872
873
874
875
876
877
878
879
880
881
882
883
884

extraction and real-time RT-PCR analysis; cells used; multicellular spheroids (MCS); TUNEL assay and FACS analysis of apoptosis; DNA content analysis and chromosome spread; confocal imaging and time-lapse videomicroscopy; analysis of mitotic defects; and immunohistochemistry. Statistical analyses were done using JMP-7 and GraphPad Prism6 softwares. The association between clinicopathological characteristics and pathological response after neoadjuvant chemotherapy were calculated using the chi-squared and the Fisher exact tests. The association between pathological response and multiple biomarkers was evaluated by a logistic regression model using categorical and continuous variables. Dot plot analyses were done using Mann-Whitney test. Data in bar graphs (mean \pm SD) were analyzed using 2-tail unpaired Student t test. $P < 0.05$ was considered statistically significant.

1. Teshome M, Hunt KK. Neoadjuvant Therapy in the Treatment of Breast Cancer. *Surg Oncol Clin N Am.* **23**, 505–523 (2014).
2. Mauri D, Pavlidis N, Ioannidis JPA. Neoadjuvant Versus Adjuvant Systemic Treatment in Breast Cancer: A Meta-Analysis. *J Natl Cancer Inst.* **97**, 188–194 (2005).
3. Van de Wiel M, Dockx Y, Van den Wyngaert T, Stroobants S, Tjalma WAA, Huizing MT. Neoadjuvant systemic therapy in breast cancer: Challenges and uncertainties. *Eur J Obstet Gynecol Reprod Biol.* **210**, 144–156 (2017).
4. Gralow JR, Burstein HJ, Wood W, Hortobagyi GN, Gianni L, von Minckwitz G, et al. Pre-operative Therapy in Invasive Breast Cancer: Pathologic Assessment and Systemic Therapy Issues in Operable Disease. *J Clin Oncol.* **26**, 814–819 (2008).
5. von Minckwitz G, Untch M, Blohmer J-U, Costa SD, Eidtmann H, Fasching PA, et al. Definition and Impact of Pathologic Complete Response on Prognosis After Neoadjuvant Chemotherapy in Various Intrinsic Breast Cancer Subtypes. *J Clin Oncol.* **30**, 1796–1804 (2012).
6. Valet F, de Cremoux P, Spyrtatos F, Servant N, Dujaric ME, Gentien D, et al. Challenging single- and multi-probesets gene expression signatures of pathological complete response to neoadjuvant chemotherapy in breast cancer: Experience of the REMAGUS 02 phase II trial. *The Breast.* **22**, 1052–1059 (2013).
7. Wang-Lopez Q, Chalabi N, Abrial C, Radosevic-Robin N, Durando X, Mouret-Reynier MA, et al. Can pathologic complete response (pCR) be used as a surrogate marker of survival after neoadjuvant therapy for breast cancer? *Crit Rev Oncol Hematol.* **95**, 88–104 (2015).
8. von Minckwitz G, Fontanella C. Comprehensive Review on the Surrogate Endpoints of Efficacy Proposed or Hypothesized in the Scientific Community Today. *J Natl Cancer Inst Monogr.* **51**, 29–31 (2015).
9. de Gramont A, Watson S, Ellis LM, Rodon J, Tabernero J, de Gramont A, et al. Pragmatic issues in biomarker evaluation for targeted therapies in cancer. *Nat Rev Clin Oncol.* **12**, 197–212 (2014).
10. Chen J-G, Horwitz SB. Differential mitotic responses to microtubule-stabilizing and -destabilizing drugs. *Cancer Res.* **62**, 1935–1938 (2002).
11. Weaver BA. How Taxol/paclitaxel kills cancer cells. *Mol Biol Cell.* **25**, 2677–2681 (2014).
12. White D, Honoré S, Hubert F. Exploring the effect of end-binding proteins and microtubule targeting chemotherapy drugs on microtubule dynamic instability. *J Theor Biol.* **429**, 18–34 (2017).
13. Zasadil LM, Andersen KA, Yeum D, Rocque GB, Wilke LG, Tevaarwerk AJ, et al. Cytotoxicity of paclitaxel in breast cancer is due to chromosome missegregation on multipolar spindles. *Sci Transl Med.* **6**, 229 (2014).
14. Petry S. Mechanisms of mitotic spindle assembly. *Annu Rev Biochem.* **85**, 659–683 (2016).
15. Prosser SL, Pelletier L. Mitotic spindle assembly in animal cells: a fine balancing act. *Nat Rev Mol Cell Biol.* **18**, 187–201 (2017).
16. Rouzier R, Rajan R, Wagner P, Hess KR, Gold DL, Stec J, et al. Microtubule-associated protein tau: a marker of paclitaxel sensitivity in breast cancer. *Proc Natl Acad Sci U S A.* **102**, 8315–8330 (2005).
17. Andre F, Hatzis C, Anderson K, Sotiriou C, Mazouni C, Mejia J, et al. Microtubule-associated protein-tau is a bifunctional predictor of endocrine sensitivity and chemotherapy resistance in estrogen receptor-positive breast cancer. *Clin Cancer Res.* **13**, 2061–2067 (2007).
18. Wang K, Deng QT, Liao N, Zhang GC, Liu YH, Xu FP, et al. Tau expression correlated with breast cancer sensitivity to taxanes-based neoadjuvant chemotherapy. *Tumour Biol.* **34**, 33–38 (2013).
19. Zhou J, Qian S, Li H, He W, Tan X, Zhang Q, et al. Predictive value of microtubule-associated protein Tau in patients with recurrent and metastatic breast cancer treated with taxane-containing palliative chemotherapy. *Tumour Biol.* **36**, 3941–3947 (2015).

Acknowledgements

We thank the members of the REMAGUS02 and REMAGUS04 groups for their contribution to this work. We thank K. Tran-Perennou for excellent technical assistance. We are grateful to Dr. Sophie Hamy-Petit (Institut Curie, Paris) for helpful discussion. This work has benefited from the facilities and expertise of the Imaging and Cytometry Platforms (Frederic De Leeuw, Yann Lecluse), UMS 3655/US23, of the Gustave Roussy Cancer Campus, Villejuif, France. **Financial support** This work has been funded by Gustave Roussy, the ANR grant MMO ANR-10-IBHU-0001, the Taxe d'Apprentissage TA2018 (University Paris Saclay, France), the Comité Ile-de-France of the Ligue Nationale contre le Cancer, the Ligue contre le Cancer 94/Val-de-Marne, the GEFLUC Ile-de-France, the Fondation ARC, CNRS, INSERM, the Fonds de Dotation Agnès b., the association Odysea and Prolific **Conflict of interest statement:** Authors declare no potential conflict of interest.

20. Baquero MT, Lostritto K, Gustavson MD, Bassi KA, Appia F, Camp RL, et al. Evaluation of prognostic and predictive value of microtubule associated protein tau in two independent cohorts. *Breast Cancer Res.* **13**, R85-R102 (2011).
21. Bonneau C, Gurard-Levin ZA, Andre F, Pusztai L, Rouzier R. Predictive and Prognostic Value of the Tau Protein in Breast Cancer. *Anticancer Res.* **35**, 5179–5184 (2015).
22. Di Benedetto M, Bièche I, Deshayes F, Vacher S, Nouet S, Collura V, et al. Structural organization and expression of human MTUS1, a candidate 8p22 tumor suppressor gene encoding a family of angiotensin II AT2 receptor-interacting proteins. *ATIP. Gene.* **380**, 127–136 (2006).
23. Rodrigues-Ferreira S, Nahmias C. An ATIPical family of angiotensin II AT2 receptor-interacting proteins. *Trends Endocrinol Metab.* **21**, 684–690 (2010).
24. Rodrigues-Ferreira S, Di Tommaso A, Dimitrov A, Cazaubon S, Gruel N, Colasson H, et al. 8p22 MTUS1 Gene Product ATIP3 Is a Novel Anti-Mitotic Protein Underexpressed in Invasive Breast Carcinoma of Poor Prognosis. *PLoS ONE.* **4**, e7239 (2009).
25. Molina A, Velot L, Ghouinem L, Abdelkarim M, Bouchet BP, Luissint A-C, et al. ATIP3, a Novel Prognostic Marker of Breast Cancer Patient Survival, Limits Cancer Cell Migration and Slows Metastatic Progression by Regulating Microtubule Dynamics. *Cancer Res.* **73**, 2905–2915 (2013).
26. Marangoni E, Vincent-Salomon A, Auger N, Degeorges A, Assayag F, de Cremoux P, et al. A new model of patient tumor-derived breast cancer xenografts for preclinical assays. *Clin Cancer Res.* **13**, 3989–3998 (2007).
27. Antoni D, Burckel H, Josset E, Noel G. Three-Dimensional Cell Culture: A Breakthrough in Vivo. *Int J Mol Sci.* **16**, 5517–5527 (2015).
28. Rodrigues-Ferreira S, Nehlig A, Monchecourt C, Nasr S, Fuhrmann L, Lacroix-Triki M, et al. Combinatorial expression of microtubule-associated EB1 and ATIP3 biomarkers improves breast cancer prognosis. *Breast Cancer Res Treat.* **173**, 573–583 (2019).
29. Carter SL, Eklund AC, Kohane IS, Harris LN, Szallasi Z. A signature of chromosomal instability inferred from gene expression profiles predicts clinical outcome in multiple human cancers. *Nat Genet.* **38**, 1043–1048 (2006).
30. Bianchini G, Balko JM, Mayer IA, Sanders ME, Gianni L. Triple-negative breast cancer: challenges and opportunities of a heterogeneous disease. *Nat Rev Clin Oncol.* **13**, 674–690 (2016).
31. Basto R, Brunk K, Vinadogrova T, Peel N, Franz A, Khodjakov A, Raff JW. Centrosome amplification can initiate tumorigenesis in flies. *Cell.* **133**, 1032–1042 (2008).
32. Ganem NJ, Godinho SA, Pellman D. A mechanism linking extra centrosomes to chromosomal instability. *Nature.* **460**, 278–282 (2009).
33. Levine MS, Bakker B, Boeckx B, Moyett J, Lu J, Vitre B, et al. Centrosome amplification is sufficient to promote spontaneous tumorigenesis in mammals. *Dev Cell.* **40**, 313–322 (2017).
34. Pannu V, Mittal K, Cantuaria G, Reid MD, Li X, Donthamsetty S, et al. Rampant centrosome amplification underlies more aggressive disease course of triple negative breast cancers. *Oncotarget.* **6**, 10487–10497 (2015).
35. Denu RA, Zasadil LM, Kanugh C, Laffin J, Weaver BA, Burkard ME. Centrosome amplification induces high grade features and is prognostic of worse outcomes in breast cancer. *BMC Cancer.* **16**, 47–59 (2016).
36. Janssen A, Kops GJ, Medema RH. Elevating the frequency of chromosome mis-segregation as a strategy to kill tumor cells. *Proc Natl Acad Sci U S A.* **106**, 19108–19113 (2009).
37. Silk AD, Zasadil LM, Holland AJ, Vitre B, Cleveland DW, Weaver BA. Chromosome missegregation rate predicts whether aneuploidy will promote or suppress tumors. *Proc Natl Acad Sci U S A.* **110**, E4134–4141 (2013).
38. Vargas-Rondón N, Villegas VE, Rondón-Lagos M. The Role of Chromosomal Instability in Cancer and Therapeutic Responses. *Cancers.* **10**, e4 (2017).

885
886
887
888
889
890
891
892
893
894
895
896
897
898
899
900
901
902
903
904
905
906
907
908
909
910
911
912
913
914
915
916
917
918
919
920
921
922
923
924
925
926
927
928
929
930
931
932
933
934
935
936
937
938
939
940
941
942
943
944
945
946
947
948
949
950
951
952

Please review all the figures in this paginated PDF and check if the figure size is appropriate to allow reading of the text in the figure.

If readability needs to be improved then resize the figure again in 'Figure sizing' interface of Article Sizing Tool.